machines

MDPI

Article

Research on Gear Modification Optimization of High-Speed Heavy-Load Reducer Based on Romax

Xiao Yang [1], Xiaoping Xie [1,*], Nanquan Jiang [1], Pengchuan Wang [2] and Xuan Zhao [2]

[1] State Key Laboratory of Advanced Design and Manufacturing Technology for Vehicle, College of Mechanical and Vehicle Engineering, Hunan University, Changsha 410082, China; yangxiao011017@163.com (X.Y.); jnq@hnu.edu.cn (N.J.)
[2] Shaanxi Fast Gear Co., Ltd., Xi'an 710119, China; 00011146@fastgroup.cn (P.W.); zhaoxuan@fastgroup.cn (X.Z.)
* Correspondence: xp_xie@hnu.edu.cn

Abstract

This paper investigates the gear whine problem in a high-speed heavy-load reducer. A rigid-flexible coupled multibody dynamic model of the reducer is established using Romax. Transmission error, unit load, tooth root stress, and contact stress are used as optimization objectives. A comprehensive gear micro-modification method including lead crowning, lead slope, involute crowning, and involute slope is proposed, and a genetic algorithm is employed for optimization. The peak-to-peak transmission error [TE(p-p)] decreased from 0.27 μm to 0.19 μm for the first-stage gear pair and from 2.67 μm to 0.96 μm for the second-stage gear pair, corresponding to reductions of 29.63% and 64.04%, respectively. The maximum contact stresses decreased from 507 MPa to 488 MPa (3.75%) and from 627 MPa to 618 MPa (1.44%) for the first- and second-stage gear pairs, respectively. The radiated noise of the gearbox was reduced by about 10 dB on average. The proposed method provides a reference for the microgeometry design of high-speed heavy-load reducers.

Keywords: gear modification; high-speed heavy-load reducer; Romax; vibration and noise; transmission error

1. Introduction

Modern industry continues to advance toward high-end, intelligent, and green development. High-speed heavy-load gear transmission systems are core power-transmission components of large-scale mechanical equipment, and their performance directly affects system reliability, efficiency, and service life. Under such extreme operating conditions, gear pairs not only bear high torque loads but also generate significant dynamic excitations during high-speed operation. These excitations mainly originate from manufacturing errors, installation deviations, and elastic deformation during meshing. They lead to uneven tooth-surface load distribution and stress concentration. Consequently, vibration and noise increase, and early failures such as pitting and tooth breakage may occur [1]. Gear modification is a key approach to addressing these dynamic problems. Its fundamental principle is to introduce slight preset deviations in the tooth profile and lead, thereby compensating for meshing misalignment caused by load and deformation. This produces a more uniform load distribution along the tooth width and improves the smoothness of engagement and disengagement. As a result, vibration and noise are reduced and load-carrying capacity is improved [2].

Numerous studies on gear modification have been conducted by scholars both domestically and internationally. Raut et al. [3] experimentally investigated the effects of

Check for updates

Academic Editor: Payam Shams Ghahfarokhi

Received: 4 July 2026
Revised: 28 July 2026
Accepted: 29 July 2026
Published: 9 August 2026

Copyright: © 2026 by the authors. Licensee MDPI, Basel, Switzerland. This article is an open access article distributed under the terms and conditions of the Creative Commons Attribution (CC BY) license.

geometric parameters, including addendum height, backlash, and tip relief, on the vibration characteristics of spur gear pairs, and optimized these parameters using the Taguchi Method. Ghosh and Chakraborty [4] evaluated gear vibration and noise by measuring dynamic meshing forces as well as stress distributions in gear teeth and bearings. The optimal tooth profile modification parameters were obtained using contour plotting and a semi-analytical method. Carbonell et al. [5] calculated the dynamic response of gearboxes using a frequency iteration method, which demonstrates high accuracy in predicting structural vibration amplitudes. Bruyère and Velex [6] investigated the meshing elasticity and contact patterns of narrow-face-width spur and helical cylindrical gears. Based on theoretical analyses, they proposed a semi-analytical formulation to minimize the time-varying amplitude of transmission error by optimizing tooth profile modification and tip relief. Peng et al. [7] established a drivetrain simulation model based on the MASTA software platform. By optimizing modification parameters such as lead crowning, helix angle modification, and pressure angle of the tooth profile, the transmission error of the first-stage gear pair was effectively reduced. Li et al. [8] constructed a multibody dynamic model of a reducer based on four evaluation indices, namely transmission error, contact pattern, bearing seat stiffness, and modal characteristics. Using simulation results, they analyzed the influence of the comprehensive deformation of the reducer on gear transmission error and tooth surface contact conditions. Ultimately, the transmission error of the gear pair was reduced through tooth profile modification. Zhao et al. [9] proposed an approximate substitution method for diagonal modification, in which the micro-modification amount was used to approximate the variation in the diagonal modification slope, thereby simplifying the parameter calculation process. After applying this modification method to a two-stage reducer for a new energy vehicle, both the transmission error of the meshing gear pair and the maximum unit-length load on the tooth surface were significantly reduced [10].

This study focuses on a high-speed heavy-load reducer and adopts a research framework consisting of the following steps: experimental testing → problem identification → solution proposal → simulation optimization → experimental validation [11]. A rigid-flexible coupled multibody dynamic simulation model of the reducer is established based on Romax [12]. The optimization objectives include reducing transmission error [13], lowering unit load, tooth root stress, and contact stress, and achieving a more uniform stress distribution [14]. By integrating the Genetic Algorithm, a comprehensive gear micro-modification method is proposed, incorporating lead crowning, lead slope, involute crowning, and involute slope [15]. Ultimately, the modification parameters with the highest comprehensive score are identified. The results provide valuable reference for subsequent research on gear modification design [16].

2. Materials and Methods

2.1. Vibration and Noise Test Analysis

To avoid interference from environmental noise and ensure the accuracy of the experimental results, the reducer NVH test was conducted in a semi-anechoic chamber. Five acoustic sensors and six triaxial vibration acceleration sensors were arranged on the reducer. To ensure the reliability of data acquisition, all acoustic sensors were calibrated for sensitivity prior to installation. The schematic diagrams of the sensor arrangement are shown in Figures 1 and 2.

P1 is located on the housing at the front end of the input shaft. P2 is located at the front end of the intermediate shaft, and P3 is located at the rear end of the input shaft. P4 is located at the rear end of the output shaft, while P5 is located at the rear end of the intermediate shaft. P6 is located on the upper surface of the gearbox housing.

https://doi.org/10.3390/machines14080910

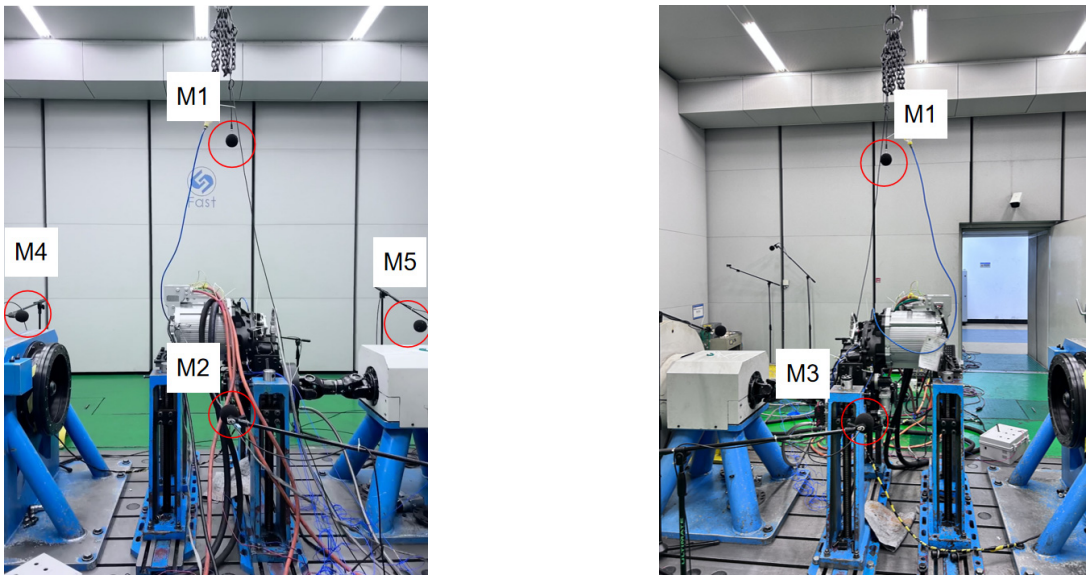


Figure 1. Layout of acoustic sensor measurement points.

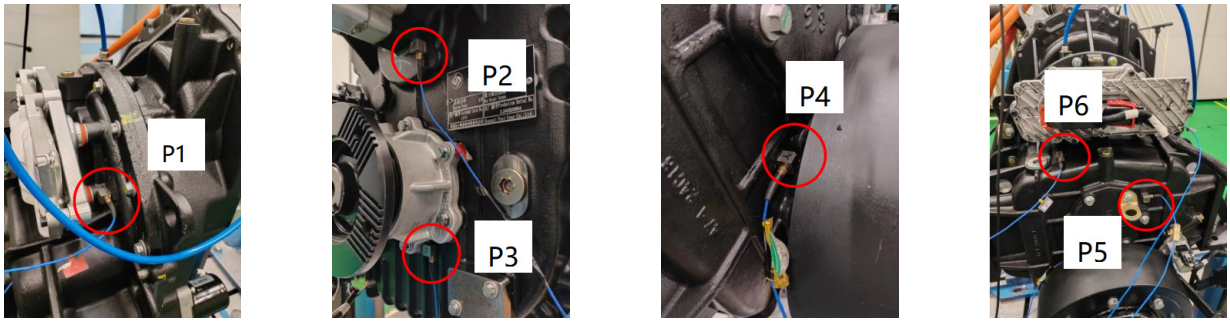


Figure 2. Layout of velocity sensor measurement points.

The vibration and noise tests used an LMS SCADAS Mobile portable multichannel data acquisition system with 12 acquisition channels. Signal acquisition and post-processing were performed using LMS Test.Lab 17A. The test equipment and acquisition parameters are summarized in Table 1, and the signal acquisition and analysis workflow is shown in Figure 3.

Table 1. Test equipment and acquisition parameters.

Item	Configuration/Quantity	Main Parameters
Reducer test	One two-stage reducer	No-load run-up; 500–9000 r/min; 50 r/min/s; 170 s; oil temperature 80 ± 5 °C
Triaxial accelerometers	Six PCB triaxial sensors	±50 g; 0.5–5 kHz; 100 mV/g; −55 to +125 °C
Free-field microphones	Five PCB free-field sensors; Larson Davis CAL200 calibrator	30–143 dB; 3.15–20 kHz; 50 mV/Pa; −30 to +85 °C; 1 m; 94/114 dB calibration
Acquisition and analysis	LMS SCADAS Mobile; 12 channels; LMS Test.Lab 17A	Order analysis over 2000–7500 r/min

For the reducer system under investigation, the gear-meshing orders were first determined. With the input shaft selected as the reference shaft, the order is defined as the ratio of a signal frequency to the rotational frequency of the reference shaft [10]:

$$O = 60\,f/n \quad (1)$$

In Equation (1), O is the dimensionless order, f is the signal frequency in Hz, and n is the rotational speed of the reference shaft in r/min.

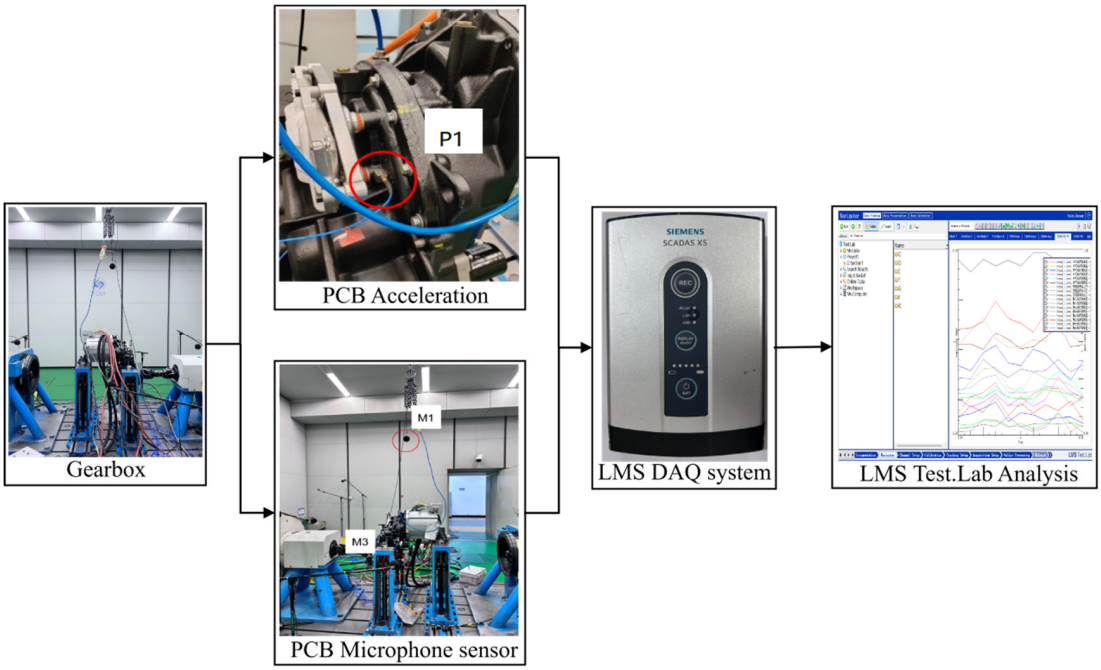


Figure 3. Vibration and noise acquisition, analysis, and processing workflow.

Based on Equation (1) and the gear parameters listed in Table 2, the meshing orders of the two gear pairs were calculated, as shown in Table 3.

Table 2. Gear parameters.

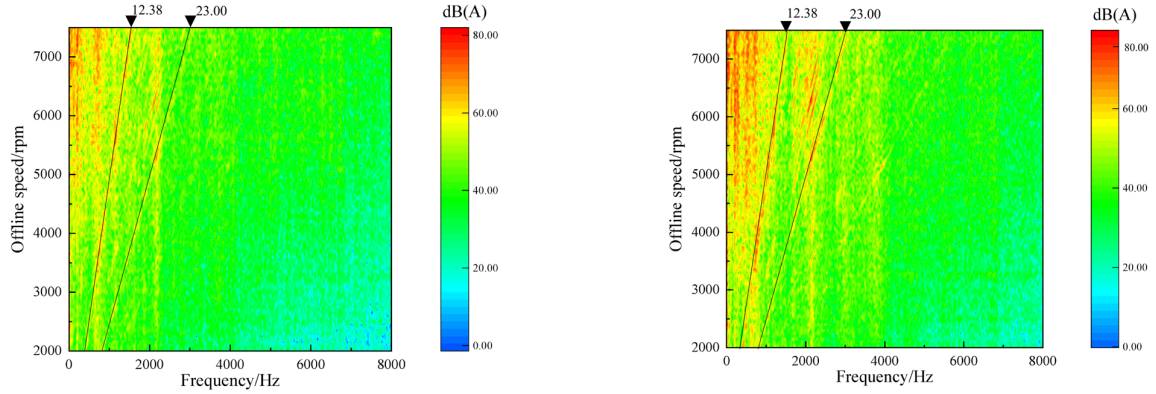
Gear	Number of Teeth
Driving gear on input shaft	23
Driven gear on intermediate shaft	78
Driving gear on intermediate shaft	42
Driven gear on output shaft	43

Table 3. Meshing orders of the gear pairs.

Component	Order
First-stage gear pair	23.00
Second-stage gear pair	12.38

During the test, significant gear whine was observed during operation. To further analyze the gear whine and its causes, the noise signals were subjected to order analysis using LMS Test.Lab 17A. The colormap of the noise at the near-field measurement points of the gearbox was obtained. Due to space limitations, the order analysis results of the M1 and M2 acoustic sensors are presented in Figure 4.

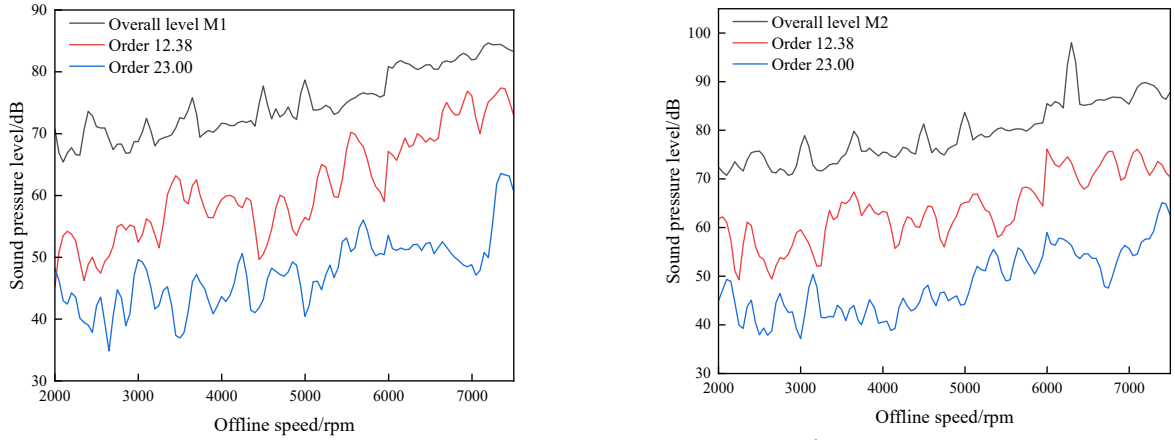
As shown in Figure 4, obvious order-related noise occurs as the input-shaft speed increases from 2000 to 7500 r/min. The 23rd-order and 12.38th-order components are particularly evident. According to the gear parameters and order-tracking relationship, the 23rd order corresponds to the first-stage gear-meshing frequency, whereas the 12.38th order corresponds to the second-stage gear-meshing frequency. Order slices were then extracted to compare these components with the overall noise level.



(**a**) Acoustic sensor M1 (**b**) Acoustic sensor M2

Figure 4. Noise colormaps at selected near-field measurement points of the gearbox.

Figure 5 shows that the 12.38th-order component makes a substantial contribution to the overall noise level. Therefore, the second-stage gear pair was selected as the primary target for optimization.



(**a**) Acoustic sensor M1 (**b**) Acoustic sensor M2

Figure 5. Order noise and overall noise for acoustic sensors M1 and M2.

2.2. Reducer Modeling and Simulation

To ensure computational efficiency, rapid convergence, and uncompromised calculation accuracy, the gearbox housing was meshed using Altair HyperMesh 2022. During the flexibility modeling of the housing, structural features such as fillets were considered to have a negligible effect on vibration and noise and were therefore simplified. The entire housing model was discretized using tetrahedral elements, with the element type set as C3D8R. The final meshed model consisted of 748,986 elements, as shown in Figure 6.

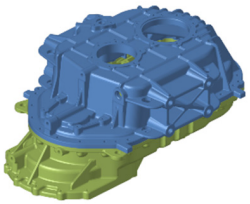


Figure 6. Finite element model of the housing.

A gear-transmission model of the reducer was established in Romax Designer 2023.1, including the gears, bearings, and gear shafts. Material properties and connection relationships were assigned to the housing finite element model developed in HyperMesh. The

housing model was then imported into Romax to establish the rigid-flexible coupled model shown in Figure 7.

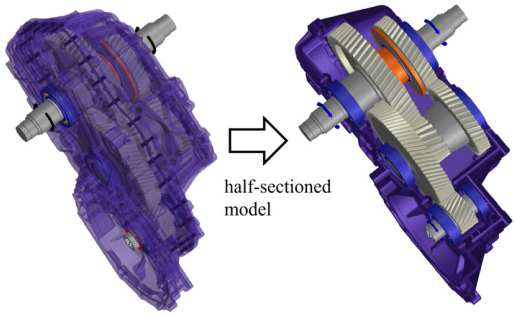


Figure 7. Rigid-flexible coupled model of the reducer.

2.3. Gear Micro-Modification Optimization

This study focuses on the analysis and optimization of second-stage gear whine. The analysis condition was set to an input speed of 8400 r/min and a torque of 140 N·m. The established rigid-flexible coupled model was used to evaluate both gear pairs under this condition. Before microgeometry optimization, the maximum and minimum transmission errors of the first-stage gear pair were 0.13 μm and −0.14 μm, giving a TE(p-p) of 0.27 μm. The corresponding values for the second-stage gear pair were 1.34 μm and −1.33 μm, giving a TE(p-p) of 2.67 μm.

Before microgeometry optimization, the maximum tooth-surface contact stresses of the first- and second-stage gear pairs were 507 MPa and 627 MPa, respectively.

The bearing dynamic forces induced by transmission error were applied to the bearing housings as excitation. A boundary-element acoustic model of the reducer housing exterior surface was established in Simcenter 3D 2306. A spherical measurement field with a radius of 1 m was created, and six field points were selected to extract the sound pressure responses. Their locations are shown in Figure 8.

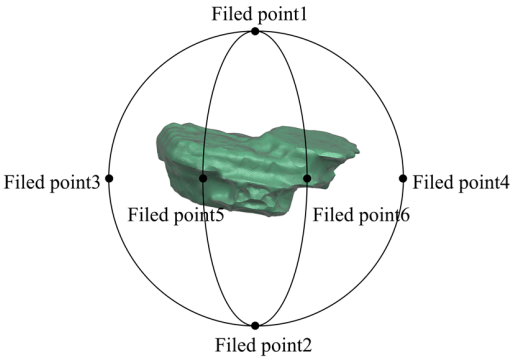


Figure 8. Sound pressure field points.

The sound pressure responses at the six field points were analyzed over 100–5000 Hz, as shown in Figure 9. The radiated noise generally increases and then decreases with frequency. The main peaks occur between 2000 and 3000 Hz, and the maximum sound pressure level reaches approximately 100 dB.

Lead modification is used to reduce gear noise and uneven tooth-surface load distribution. It mainly includes lead crowning and lead slope modification. The tangential force, equivalent mesh stiffness, and lead crowning amount were determined using Equations (2)–(4), respectively [17,18]:

$$F_m = \frac{2T}{d} \tag{2}$$

$$C_r = (0.75\varepsilon_\alpha + 0.25C^*) \tag{3}$$

$$C_e = (2 \sim 3)\frac{F_m}{bC_r} \tag{4}$$

In the equation, F_m represents the tangential force at the pitch circle, T is the torque, d is the pitch circle diameter, C_r is the equivalent stiffness of the gear pair, C^* is the single-pair tooth stiffness, ε_α is the facewidth overlap ratio, b is the tooth width, and C_e is the lead crowning amount.

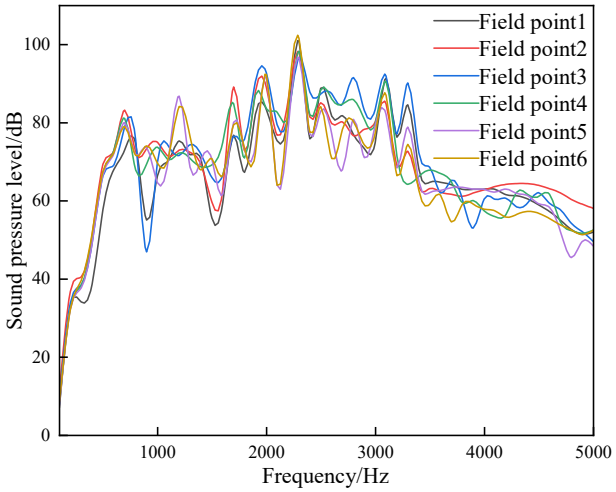


Figure 9. Radiated sound pressure curves at the six field points.

The maximum lead slope modification was determined using Equation (5) [19]:

$$C_h = F_{\beta y} - \frac{F_m}{bC_r} \tag{5}$$

In the equation, C_h represents the lead slope modification amount, and $F_{\beta y}$ denotes the meshing misalignment angle.

The involute crowning amount was determined using Equation (6) [20]:

$$C = \frac{F_A K_{mp} F_t}{b \cos \alpha_t C_r} \tag{6}$$

In the equation, K_A is the usage factor 1, K_{mp} is the branch factor, α_t is the facewidth pressure angle, and C is the involute crowning amount.

The maximum involute slope modification was determined using the N·Sigg expression in Equation (7) [20]:

$$A = (4 + 0.04\frac{F_t}{b_{ca}}) \pm 4 \tag{7}$$

In the equation, b_{ca} represents the effective contact width of the gear, and A denotes the involute slope.

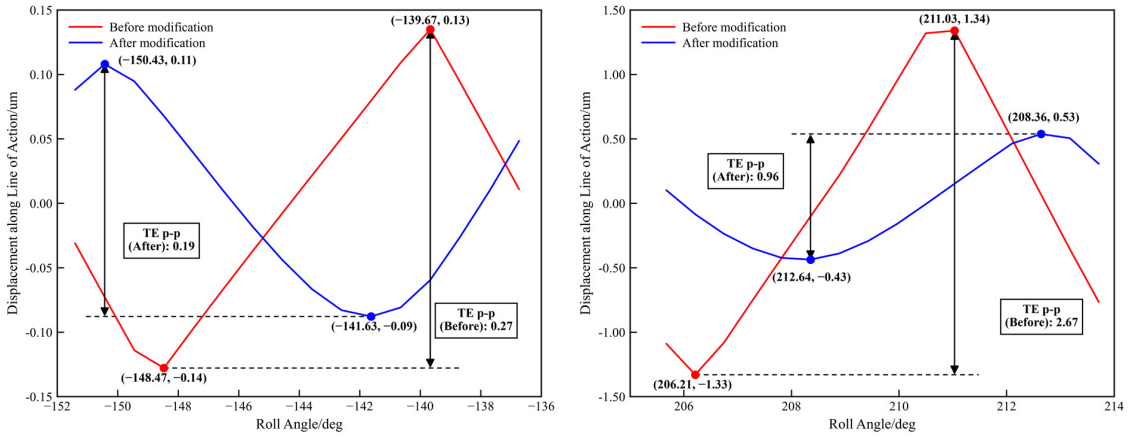
In the Romax model, lead crowning, lead slope, involute crowning, and involute slope were applied to the working flanks of both gear stages. To account for thermal deformation and related effects, the crowning amount was constrained to remain positive, with a lower bound of 2 μm. The remaining parameter ranges were determined using Equations (2)–(7). The optimized parameters are listed in Table 4.

Table 4. Optimized gear microgeometry parameters.

Modification Variable (μm)	First-Stage Driving Gear	First-Stage Driven Gear	Second-Stage Driving Gear	Second-Stage Driven Gear
Lead Crowning	9.82	5.00	2.58	5.48
Lead Slope	12.71	2.03	5.50	2.04
Involute Crowning	10.00	10.00	8.06	8.64
Involute Slope	0.00	0.00	10.50	6.51

3. Results and Discussion

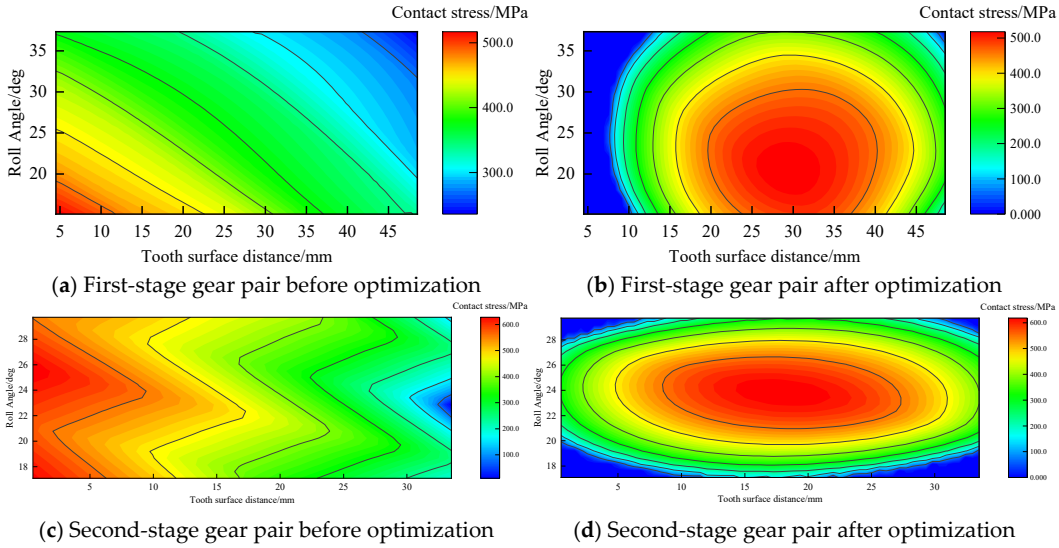
The optimal microgeometry parameters obtained using the genetic algorithm were applied to the reducer model. As shown in Figure 10, the TE(p-p) of the first-stage gear pair decreased from 0.27 μm to 0.19 μm, a reduction of 29.63%. For the second-stage gear pair, TE(p-p) decreased from 2.67 μm to 0.96 μm, corresponding to a reduction of 64.04%.



(**a**) First-stage gear pair (**b**) Second-stage gear pair

Figure 10. Transmission error before and after microgeometry optimization.

As shown in Figure 11, the tooth-surface load distribution became more uniform after microgeometry optimization. The maximum contact stress of the first-stage gear pair decreased from 507 MPa to 488 MPa, a reduction of 3.75%. The corresponding value for the second-stage gear pair decreased from 627 MPa to 618 MPa, a reduction of 1.44%.

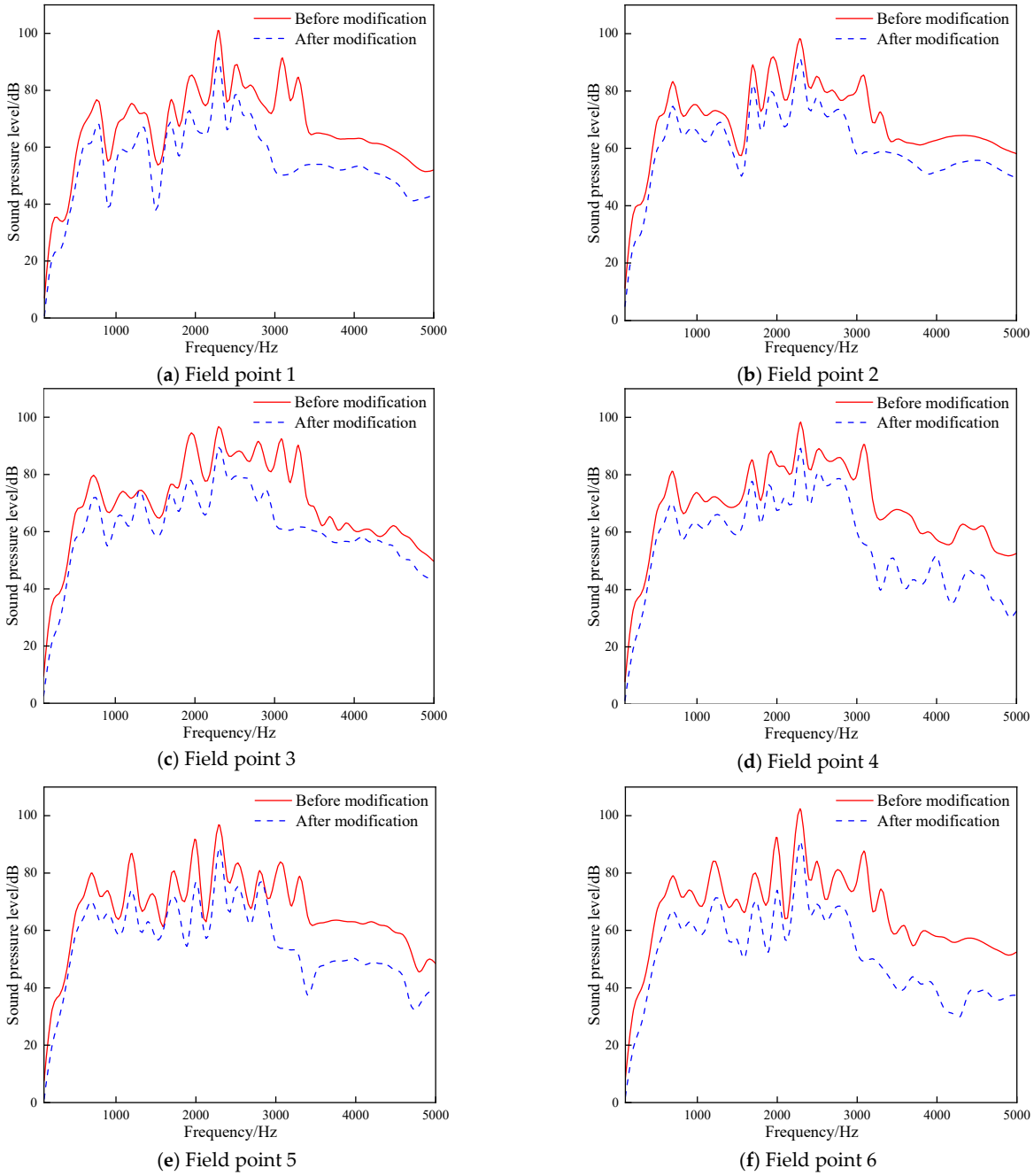


(**a**) First-stage gear pair before optimization (**b**) First-stage gear pair after optimization

(**c**) Second-stage gear pair before optimization (**d**) Second-stage gear pair after optimization

Figure 11. Maximum contact stress contours before and after microgeometry optimization.

Figure 12 and Table 5 compare the radiated sound pressure responses at the six field points before and after microgeometry optimization. The reduction is particularly evident in the 3000–5000 Hz range. The average maximum sound pressure level at the field points decreased by approximately 10 dB, indicating improved radiated-noise performance of the reducer housing.



(**a**) Field point 1 (**b**) Field point 2

(**c**) Field point 3 (**d**) Field point 4

(**e**) Field point 5 (**f**) Field point 6

Figure 12. Sound pressure curves at the six field points before and after microgeometry optimization.

Table 5. Maximum sound pressure levels before and after microgeometry optimization.

	Field Point 1	Field Point 2	Field Point 3	Field Point 4	Field Point 5	Field Point 6
Before modification (dB)	100.89	98.03	96.74	98.34	96.69	101.65
After modification (dB)	90.40	89.19	89.49	89.21	88.97	90.94
Reduction (dB)	10.49	8.84	7.25	9.13	7.72	10.71

4. Conclusions

This study, combining engineering practice, analyzed and optimized the gear whine problem in a high-speed heavy-load reducer, leading to the following conclusions:

1. A transmission model of the gearbox was established in Romax. With transmission error and unit-length surface load as optimization objectives, a comprehensive gear micro-modification method was developed using four design parameters and a genetic algorithm.
2. After microgeometry optimization, the TE(p-p) values of the first- and second-stage gear pairs were reduced by 29.63% and 64.04%, respectively. The contact patterns became more uniform, and localized loading was alleviated.
3. The radiated noise of the gearbox housing was simulated using Simcenter 3D. Reducing the transmission excitation through gear micro-modification lowered the maximum radiated sound pressure by up to 10 dB, providing a basis for further improvement of reducer NVH performance.

Author Contributions: Conceptualization, X.Y. and X.X.; methodology, X.Y. and N.J.; software, X.Y.; validation, X.Y., P.W. and X.Z.; formal analysis, X.Y.; investigation, X.Y., P.W. and X.Z.; resources, P.W. and X.Z.; data curation, X.Y. and P.W.; writing—original draft preparation, X.Y.; writing—review and editing, X.X., N.J., P.W. and X.Z.; visualization, X.Y.; supervision, X.X. and N.J.; project administration, X.X.; funding acquisition, X.X. All authors have read and agreed to the published version of the manuscript.

Funding: This work was supported by the National Key R&D Program of China (Grant number 2023YFB3406500). It was also supported by the Hunan Key Laboratory of Automotive Power and Transmission Systems (VPTS202302).

Institutional Review Board Statement: Not applicable.

Informed Consent Statement: Not applicable.

Data Availability Statement: The datasets presented in this article are not publicly available because they are subject to confidentiality requirements of the industrial collaborative project.

Conflicts of Interest: Authors Pengchuan Wang and Xuan Zhao were employed by Shaanxi Fast Gear Co., Ltd. The remaining authors declare that the research was conducted in the absence of any commercial or financial relationships that could be construed as a potential conflict of interest. The funding sponsors had no role in the design of the study; in the collection, analyses, or interpretation of data; in the writing of the manuscript; or in the decision to publish the results.

References

1. Wen, B. *Mechanical Design Handbook*, 5th ed.; China Machine Press: Beijing, China, 2010; Volume 3.
2. Litvin, F.L.; Fuentes, A. *Gear Geometry and Applied Theory*; Cambridge University Press: Cambridge, UK, 2004.
3. Raut, A.S.; Kumar, M.S.; Gopal, V.S. Optimization of Geometrical Features of Spur Gear Pair Teeth for Minimization of Vibration Generation. *J. Vib. Eng. Technol.* **2023**, *12*, 533–545. [CrossRef]
4. Ghosh, S.S.; Chakraborty, G. On optimal tooth profile modification for reduction of vibration and noise in spur gear pairs. *Mech. Mach. Theory* **2016**, *105*, 145–163. [CrossRef]
5. Carbonell, A.; Rigaud, E.; Perret, L. Vibroacoustic Analysis of Geared Systems: Predicting and Controlling the Whining Noise. In *Automotive NVH Technology*; Springer International Publishing: Berlin, Germany, 2016; pp. 63–79.
6. Bruyere, J.; Velex, P. Towards General Performance Diagrams to Define Optimum Profile and Lead Modifications with Regard to Transmission Error in Spur and Helical Gears. *Mech. Mach. Theory* **2022**, *176*, 105021.
7. Peng, Z.; Liu, J.; Xiong, F.; Wei, D. Study on Gear Whine of Hybrid Powertrain Systems Based on Contact Pattern and Micro-Geometry Modification. *Mech. Transm.* **2020**, *44*, 14–20. [CrossRef]
8. Li, Q.; Li, J.; Liu, J.; Li, Y.; Zhao, H. NVH Simulation and Optimization of Electric Vehicle Reducers. *Mech. Transm.* **2022**, *46*, 107–113.

9. Zhao, M.; Chen, Z.; Tang, Z.; Wang, M.; Zheng, X.; Sun, J. Noise Reduction Study of Two-Stage Reducer Gears for New Energy Vehicles Based on Diagonal Modification. *Sci. Technol. Eng.* **2020**, *20*, 9354–9361.
10. Shi, Z.; Liu, S.; Yue, H.; Wu, X. Noise analysis and optimization of the gear transmission system for two-speed automatic transmission of pure electric vehicles. *Mech. Sci.* **2023**, *14*, 333–345. [CrossRef]
11. Yang, H.; Shi, W.; Xu, M.; Yang, X.; Yang, D.; Xin, L. Analysis and control of gearbox whine of a heavy commercial vehicle based on planet phasing theory and bench test. *Proc. Inst. Mech. Eng. Part K J. Multi-Body Dyn.* **2025**, *239*, 214–233. [CrossRef]
12. Im, D.; Chung, W.-J.; Lee, H.; Lee, Y.-J.; Sung, H.; Lee, M.; Park, Y.-J. Analysis of gear transmission error in helical gear using enhanced tooth contact analysis model considering measured tooth profile errors. *Sci. Rep.* **2025**, *15*, 5981. [CrossRef] [PubMed]
13. Dai, L.; Liu, Y.; Jia, Y.; Zhou, W.; Zhang, A. Research on gear whine evaluation method based on transmission error sensitivity. *J. Phys. Conf. Ser.* **2024**, *2827*, 012024. [CrossRef]
14. Cianciotta, L.; Cirelli, M.; Valentini, P.P. Multi-objective optimization of gear design of E-Axles to improve noise emission and load distribution. *Machines* **2025**, *13*, 330. [CrossRef]
15. Mohammed, O.D.; Bhat, A.D.S.; Falk, P. Robust multi-objective optimization of gear microgeometry design. *Simul. Model. Pract. Theory* **2022**, *119*, 102593. [CrossRef]
16. Chung, W.J.; Park, Y.J.; Choi, C.; Kim, S.C. Effects of manufacturing errors of gear macro-geometry on gear performance. *Sci. Rep.* **2023**, *13*, 50. [CrossRef] [PubMed]
17. *GB/T 3480-1997*; Calculation Method for the Load Capacity of Involute Cylindrical Gears. The Standardization Administration of the People's Republic of China: Beijing, China, 1997.
18. Li, R. *Stiffness Analysis and Modification Methods of Gear Transmission*; Chongqing University Press: Chongqing, China, 1998; pp. 266–268.
19. Ge, R.; Jiang, X.; Yang, W. Application of Tooth Surface Micro-Modification in Noise Reduction of Automotive Gearboxes. *Automot. Eng.* **2009**, *31*, 557–560.
20. Tian, D.; Li, J.; Tao, L.; Zhou, C. Gear Modification Design of Megawatt Wind Power Accelerators Based on Romax. *Wind Energy* **2021**, *10*, 70–75.

Disclaimer/Publisher's Note: The statements, opinions and data contained in all publications are solely those of the individual author(s) and contributor(s) and not of MDPI and/or the editor(s). MDPI and/or the editor(s) disclaim responsibility for any injury to people or property resulting from any ideas, methods, instructions or products referred to in the content.